Front. Optoelectron. China 2011, 4(2): 176–180
DOI 10.1007/s12200-011-0160-y

RESEARCH ARTICLE

High-yield synthesized silver orthophosphate nanowires and their application in photoswitch

Ronghui QUE (✉)

Anhui Key Laboratory of Functional Molecular Solids, College of Chemistry and Materials Science, Anhui Normal University, Wuhu 241000, China

Abstract Large-scale, high-purity and uniform silver orthophosphate (Ag_3PO_4) nanowires had been synthesized by a facile hydrothermal method without employing any surfactants or templates for the first time. The nanowires were single-crystalline with lengths up to several micrometers. X-ray diffraction, scanning electron microscopy, transmission electron microscopy, and high-resolution transmission electron microscopy were used to characterize the morphology and structure of the as-prepared products. The as-prepared Ag_3PO_4 nanowires exhibited linear current-voltage (*I-V*) characteristics and excellent photoresponse. As the light was switched on and off, the currents could be reversibly switched between high and low value at the voltage of 0.1 V, which will find wide application in optoelectronic nanodevices.

Keywords Ag_3PO_4 nanowires, hydrothermal reaction, photoswitch

1 Introduction

One-dimensional (1D) semiconductors with well-controlled size, morphology, and chemical composition have been the focus of scientific research due to their unique chemical-physical properties and potential applications in electrons, photonics, chemical sensing, and biological imaging [1–6]. To date, a wide range of materials have been prepared in the form of 1D nanomaterial by a variety of methods [7–9]. Among them, various functional nanowires are a hot topic and have been successfully synthesized and applied in different fields, such as nanolasers [2], nanocatalytic [7], and nanosensors [10–13].

Silver based ionic conductors, such as Ag_2S and AgI, have served as model compounds in studies on ion and electron transport/transfer in solid-state physics [14,15]. $AgVO_3$, $Ag_xV_2O_5$, and $Ag_2V_4O_{11}$ are the most commonly occurring phases in the solid state, and the detailed structural and phase analysis on them had been widely investigated [16]. Silver molybdate/chromate are an important family of inorganic materials, which have wide potential applications in various fields. Yu et al. have successfully prepared Ag_2MoO_4, $Ag_6Mo_{10}O_{33}$, and $Ag_2Mo_2O_7$ nanoribbons [17]; Li et al. have synthesized Ag_2CrO_4 nanorods. These works are all labeled as important and valuable [18]. Our group also synthesized 1D Ag_2MO_4 (M = Cr, Mo, and W) nanomaterials through the modified hydrothermal method, and the photoresponse of the nanomaterials were also investigated [19]. Attention was also devoted to inserting other anions into these compounds to obtain new materials with high conductivities.

Today, phosphate salts have attracted great attention due to the variety of their applications in the electrical, optical, prosthetics, structural fields, etc. [20]. Also, transition metal phosphates are important as they are used as inorganic and biomaterials finding applications as catalysts, ion exchangers and in low thermal expansion ceramic materials [21]. Cutroni et al. have conducted studies on ionic conduction and dielectric behavior of Ag_3PO_4 glasses [22,23]. George studied the characterization of nano-Ag_3PO_4, and found that the nano-Ag_3PO_4 is a directric relaxor material of high dielectric constant [24]. However, the Ag_3PO_4 nanowires have not been reported.

In this paper, for the first time, Ag_3PO_4 nanowires with the width of 100 nm and the length up to several micrometers were obtained via a simple hydrothermal route without any surfactant or template. The current-voltage (*I-V*) characteristics of Ag_3PO_4 nanowires and the photoswitching response were also investigated, and we believe it will be widely used in nanodevices.

Received November 15, 2010; accepted November 30, 2010

E-mail: qrhui123@mail.ahnu.edu.cn

2 Experiment

2.1 Preparation of Ag_3PO_4 nanowires

All of the chemical regents used in our experiments were of analytical grade and without further purification. Aqueous solutions were prepared using distilled water.

In a typical procedure, 0.5 mM $AgNO_3$ and 0.25 mM Na_3PO_4 were dissolved in 25 mL distilled water, respectively. Then the $AgNO_3$ solution was added into Na_3PO_4 solution slowly under magnetic stirring to form a mixture at room temperature. The resulting mixture was transferred into a Teflon-lined autoclave with a capacity of 60 mL and heated to 160°C for 12 h, then cooled to room temperature naturally. The resultant was collected and washed several times with absolute ethanol and distilled water, and dried under vacuum at 60°C for 12 h.

2.2 Characterization

The phase and crystallography of the products were characterized by a Shimadzu XRD-6000 X-ray diffractometer equipped with Cu Kα radiation (λ = 0.15406 nm). A scanning rate of $0.05°\cdot s^{-1}$ was applied to record the pattern in the 2θ range of 10°–80°.

The morphologies of the products were analyzed with a FEI Quanta 200F scanning electron microscope equipped with an energy dispersive X-ray (EDX) spectroscope. Transmission electron microscopy (TEM), selected area electron diffraction (SAED) pattern and high-resolution transmission electron microscope (HRTEM) were captured with a JEOL-2010 transmission electron microscope, using an accelerating voltage of 200 kV. The photo image was taken from an Olympus optical microscope.

2.3 Measurements of photoconductive properties

The photoconductivity measurements were tracked with a CHI 620B (CHI Instruments, Chenhua Corporation, Shanghai, China) electrochemical workstation. A bundle of Ag_3PO_4 nanowires were dispersed and bridged over the ITO electrodes. Light was supplied with an incandescence lamp (12 V, 10 W).

3 Results and discussion

3.1 Crystallography and morphology

Figure 1 displays the XRD pattern of the Ag_3PO_4 obtained at the pH = 2. The diffraction peaks may be indexed as the cubic phase of Ag_3PO_4 with the calculated lattice constant a = 0.6046±0.0011 nm, which is consistent with the reported value, a = 0.6048 nm (JCPDS card No. 84-0512). No impurity is detected, indicating that the products have a high purity.

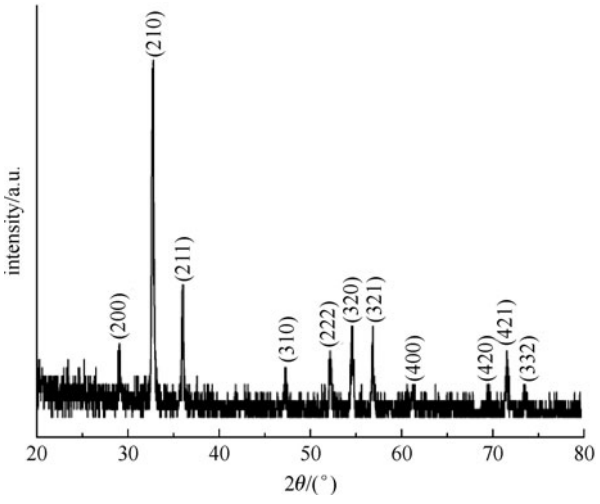

Fig. 1 XRD pattern of as-synthesized products (all diffractions peaks can be indexed as cubic Ag_3PO_4)

Field emission scanning electron microscopy (FESEM) is employed to describe the morphologies of the products. Figure 2(a) gives the low magnification image of the as-synthesized Ag_3PO_4 nanowires, with the length up to several micrometers. The high magnification shows that the diameter of the wire is about 100 nm (Fig. 2(b)). The chemical composition of these nanowires was checked by EDX in Fig. 2(b) (upper right). Besides the elements Si from the substrate, the peaks of the elements Ag, P, and O are detected in the EDX pattern.

Figure 3 shows a typical TEM image of the prepared Ag_3PO_4 nanowires, revealing the wire-like morphology features. Each wire has a uniform width along its entire length, and the average diameter is about 100 nm, which complies with the scanning electron microscopy (SEM) result. The HRTEM image (Fig. 3, inset) illustrates that the wire has lattice planes with spacing of 0.305 nm, corresponding to the d spacing of the (200) plane of the cubic phase of Ag_3PO_4 respectively. The SAED (Fig. 3, inset) taken from this area displays the crystalline structure of Ag_3PO_4, whose bright diffraction spots may be indexed as (200) and (011) respectively.

To understand the growth process of the Ag_3PO_4 nanowires, a series of parallel experiments were performed, which were checked with FESEM. When the Ag^+ came across PO_4^{3-}, it must be synthesized Ag_3PO_4 nanopaticles (Fig. 4(a)). With the hydrothermal time increased to 5 h, the wires began to grow from the center of the particle, as shown in Fig. 4(b). There are several other factors that influence the crystallinity and the morphology of Ag_3PO_4 nanowires, such as temperature and concentration. Learnt from a series of experiments, the optical reaction conditions for the synthesis of high quality Ag_3PO_4 nanowires are at 160°C for 12 h. Although the precise mechanism for the formation of Ag_3PO_4 nanowires in still under discussion, we can infer from the

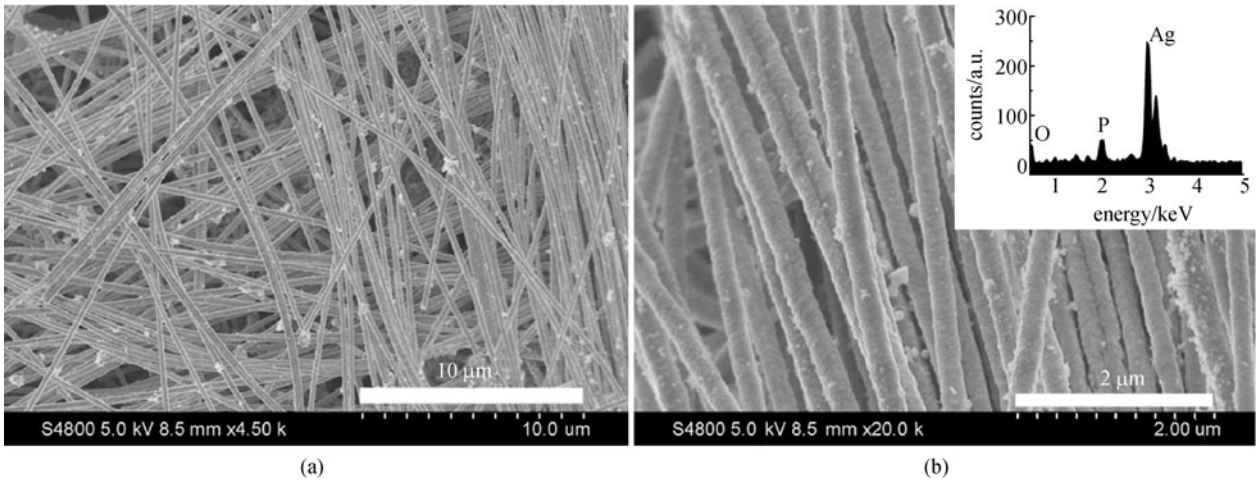

Fig. 2 SEM images revealing wires several micrometers in length and ~100 nm in diameter. (a) Low magnification; (b) high magnification and EDX spectrum (inset indicates nanowires are composed of Ag, P, and O elements)

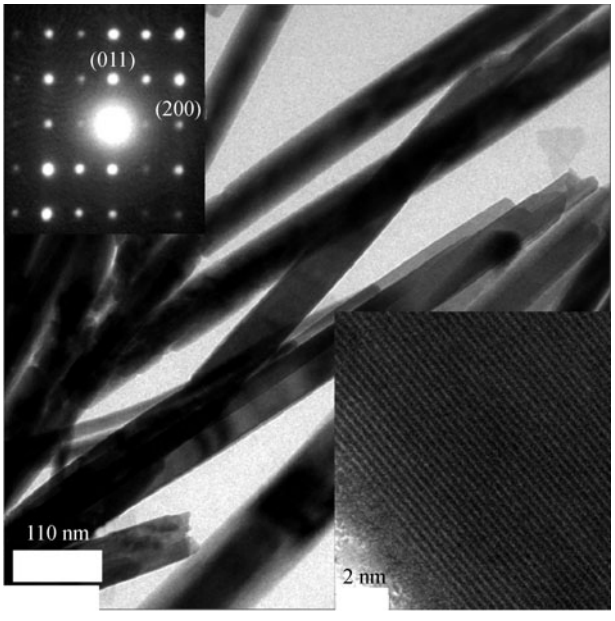

Fig. 3 TEM image of Ag_3PO_4 nanowires with diameter of 100 nm (HRTEM image of Ag_3PO_4 (low inset) shows clear crystal lattice, which can be indexed as (111) crystal planes; SAED pattern (upper inset) suggests single crystallinity of Ag_3PO_4 nanowire)

above analysis that the growth of the Ag_3PO_4 nanowires is through the solid-solution-solid transformation mechanism.

3.2 Photoswitch of Ag_3PO_4 nanowires

In order to measure the current signals through the Ag_3PO_4 nanowires, indium tin oxide (ITO) coated glass with the electrode gap of 50 μm being employed as the substrate. A bundle of Ag_3PO_4 nanowires was dispersed and bridged over the electrodes with an effective length of 60 μm, as shown in Fig. 5(a) (inset). Gold gap electrodes were fabricated on the substrate through thermal evaporation with a micrometer-sized Au wire as the mask; with a slight movement of the Au-wire mask, Au-Au gap electrodes were deposited. The distance between the wires and light source was 10 cm.

Figure 5(a) shows the *I-V* curves measured in dark (curve I) and under illumination (curve II) for comparison. Both of them exhibit a good linear behavior, which proves a fine ohmic contact between the Ag_3PO_4 nanowires and Au electrodes. The conductivity of the wires rapidly increased under illumination with an incandescence lamp. In these cases, the energy from the light excites the electrons in the ion conductor Ag_3PO_4 nanowires from the valence band into the conduction band, increasing the charge carrier concentration via direct electron-hole pair creation and thus enhancing the conductivity of the wires.

Figure 5(b) shows the reversible photoconductive characteristics of the Ag_3PO_4 nanowires. A voltage of 0.1 V was applied across the two electrodes and the current recorded during the light was alternatively on and off at 10 s intervals. Obviously, the current through the Ag_3PO_4 nanowires got promptly increased and decreased with the illumination on and off, which proves that the device is highly sensitive and are capable of repeatable activities. The measurements were performed for ten periods and proved that the photoconduction behavior was reproducible.

4 Conclusions

In summary, this work describes a facile hydrothermal method for the synthesis of large-scale, high-purity, and uniform $AgPO_4$ nanowires without employing surfactants or templates for the first time. Based on the ionic

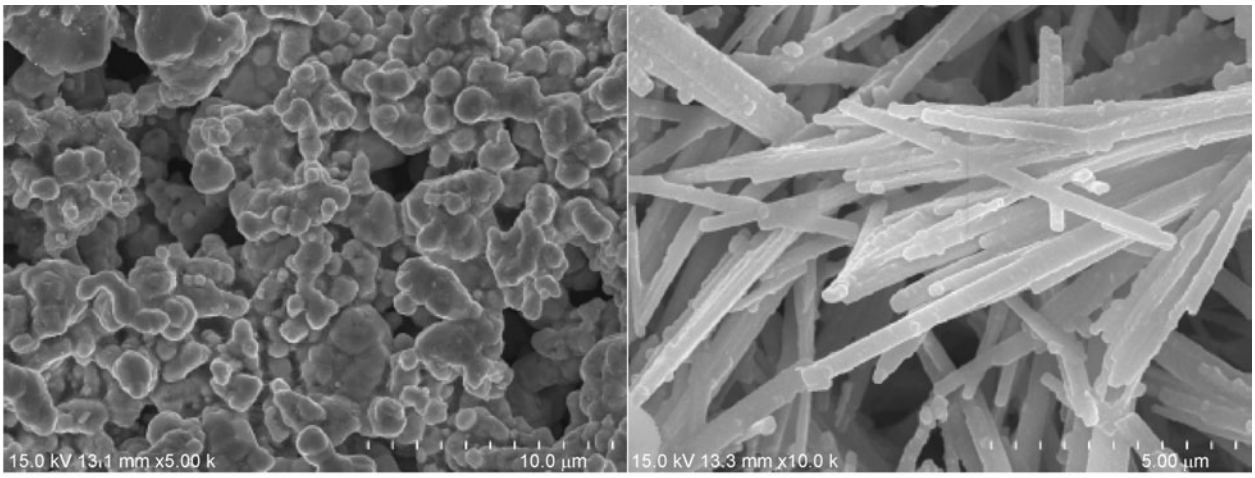

Fig. 4 SEM images of Ag_3PO_4 samples prepared after hydrothermal reaction showing morphological evolution of Ag_3PO_4 nanowires. (a) 2 h; (b) 5 h

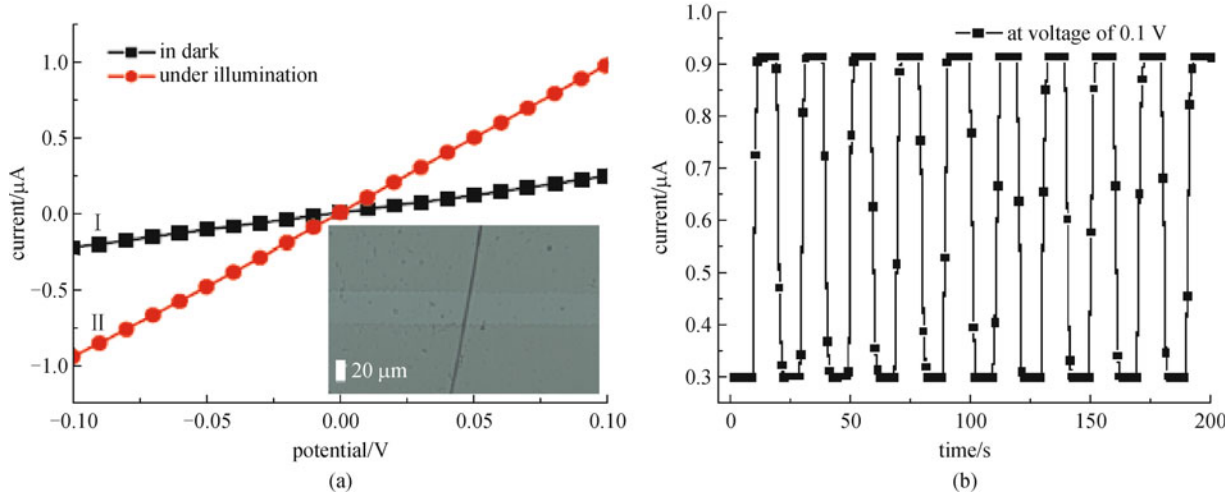

Fig. 5 Photoswitch of Ag_3PO_4 nanowires. (a) *I-V* curves of a bundle of Ag_3PO_4 nanowires measured in dark (curve I) and under illumination by using an incandescence lamp (12 V, 10 W) (curve II), and image of a bundle of Ag_3PO_4 nanowires bridging over ITO electrodes from optical microscope (inset); (b) photoconductive characteristics of device during light switching on/off (voltage of 0.1 V was applied across Au-Au electrodes and current was recorded during light alternatively on and off at 10 s intervals)

conductors of the $AgPO_4$, the as-prepared Ag_3PO_4 nanowires exhibited linear current-voltage (*I-V*) characteristics and excellent photoresponse. As the light source was switched on and off, the currents could be reversibly switched between high and low value at the voltage of 0.1 V, which will find wide applications in photo-electro nanodevices. Further work is needed in a full investigation of Ag_3PO_4 nanowires.

Acknowledgements This work was supported by the National Natural Science Foundation of China (Grant No. 21071106), and the National Basic Research Program of China (No. 2010CB934502).

References

1. Wang Z L, Song J H. Piezoelectric nanogenerators based on zinc oxide nanowire arrays. Science, 2006, 312(5771): 242–246
2. Huang M H, Mao S, Feick H, Yan H Q, Wu Y Y, Kind H, Weber E, Russo R, Yang P. Room-temperature ultraviolet nanowire nanolasers. Science, 2001, 292(5523): 1897–1899
3. Yuan G D, Zhang W J, Jie J S, Fan X, Tang J X, Shafiq I, Ye Z Z, Lee C S, Lee S T. Tunable n-Type conductivity and transport properties of Ga-doped ZnO nanowire arrays. Advanced Materials, 2008, 20 (1): 168–173

4. Shao M W, Lu L, Wang H, Wang S, Zhang M L, Ma D D D, Lee S T. An ultrasensitive method: surface-enhanced Raman scattering of Ag nanoparticles from silver vanadate and copper. Chemical Communications, 2008, (20): 2310–2312
5. Hu C G, Liu H, Dong W T, Zhang Y Y, Bao G, Lao C S, Wang Z L. $La(OH)_3$ and La_2O_3 nanobelts—synthesis and physical properties. Advanced Materials, 2007, 19(3): 470–474
6. Liu Z, Tabakman S, Welsher K, Dai H J. Carbon nanotubes in biology and medicine: *in vitro* and *in vivo* detection, imaging and drug delivery. Nano Research, 2009, 2(2): 85–120
7. Shao M W, Cheng L, Zhang X H, Ma D D D, Lee S T. Excellent photocatalysis of HF-treated silicon nanowires. Journal of the American Chemical Society, 2009, 131(49): 17738–17739
8. Shen G Z, Chen D. Self-coiling of $Ag_2V_4O_{11}$ nanobelts into perfect nanorings and microloops. Journal of the American Chemical Society, 2006, 128(36): 11762–11763
9. Mai H X, Zhang Y W, Si R, Yan Z G, Sun L D, You L P, Yan C H. High-quality sodium rare-earth fluoride nanocrystals: controlled synthesis and optical properties. Journal of the American Chemical Society, 2006, 128(19): 6426–6436
10. Kuang Q, Lao C S, Wang Z L, Xie Z X, Zheng L S. High-sensitivity humidity sensor based on a single SnO_2 nanowire. Journal of the American Chemical Society, 2007, 129(19): 6070–6071
11. Jie J S, Zhang W J, Jiang Y, Meng X M, Li Y Q, Lee S T. Photoconductive characteristics of single-crystal CdS nanoribbons. Nano Letters, 2006, 6(9): 1887–1892
12. Chen Y, Wang X H, Erramilli S, Mohanty P, Kalinowski A. Silicon-based nanoelectronic field-effect pH sensor with local gate control. Applied Physics Letters, 2006, 89(22): 223512–223513
13. Wang L Y, Yan R X, Huo Z Y, Wang L, Zeng J H, Bao J, Wang X, Peng Q, Li Y D. Fluorescence resonant energy transfer biosensor based on upconversion-luminescent nanoparticles. Angewandte Chemie, 2005, 117(37): 6208–6211
14. Tver'yanovich Y S, Balmakov M D, Tomaev W, Borisov E N, Volobueva O. Ion-conducting multilayer films based on alternating nanolayers Ag_3SI, AgI and Ag_2S, AgI. Glass Physics and Chemistry, 2008, 2(2): 150–154
15. Guo Y G, Lee J S, Maier J. AgI nanoplates with mesoscopic superionic conductivity at room temperature. Advanced Materials, 2005, 23(17): 2815–2819
16. Sharma S, Panthofer M, Jansen M, Ramanan A. Ion exchange synthesis of silver vanadates from organically templated layered vanadates. Materials Chemistry and Physics, 2005, 91(2–3): 257–260
17. Yu S H, Liu B, Mo M S, Huang J H, Liu X M, Qian Y T. General synthesis of single-crystal tungstate nanorods/nanowires: a facile, low-temperature solution approach. Advanced Functional Materials, 2003, 13(8): 639–647
18. Liang J, Peng Q, Wang X, Zheng X, Wang R J, Qiu X, Nan C W, Li Y D. Chromate nanorods/nanobelts: general synthesis, characterization, and properties. Inorganic Chemistry, 2005, 44(25): 9405–9415
19. Cheng L, Shao Q, Shao M W, Wei X W, Wu Z C. Photoswitches of one-dimensional Ag_2MO_4 (M = Cr, Mo, and W). The Journal of Physical Chemistry C, 2009, 113(5): 1764–1768
20. Cao Z, Lee B I, Samuels W D, Exarhos G J. Thermal behavior of sol-gel derived phosphate ceramics. Journal of Physics and Chemistry of Solids, 2000, 61(10): 1677–1685
21. Dinamani M, Vishnu Kamath P. Electrochemical synthesis of metal phosphates by cathodic reduction. Materials Research Bulletin, 2001, 36(11): 2043–2050
22. Cutroni M, Mandanici A, Piccolo A, Fanggao C, Saunders G A, Mustarelli P. Ionic conduction in silver phosphate glasses doped with silver sulphide. Philosophical Magazine B, 1996, 73(2): 349–365
23. Cutroni M, Mandanici A. Mechanical and dielectric behaviour of some ionic glasses. Solid State Ionics, 1998, 105(1–4): 149–157
24. Thomas M, Ghosh S K, George K C. Characterisation of nanostructured silver orthophosphate. Materials Letters, 2002, 56 (4): 386–392